



Research Article / Araştırma Makalesi

**LINEAR STATIC ANALYSIS OF LAMINATED COMPOSITE PLATES WITH
LAYERWISE FINITE ELEMENT**

Kazım Ahmet HAŞİM*, Ahmet Işın SAYGUN

Istanbul Technical University, Department of Civil Engineering, Maslak-ISTANBUL

Received/Geliş: 12.02.2014 Revised/Düzelme: 18.05.2014 Accepted/Kabul: 22.05.2014

ABSTRACT

This article is about a layerwise finite element which is developed for the linear static analysis of laminated composite plates. In the first part; the paper presents a review of the literature involving the available theories and their drawbacks for multilayered composite plates. A second part reviews a relevant keypoint (zig-zag form of the displacement field in the thickness direction) that should be considered for an accurate stress and strain field. In the third part, the paper explains the layerwise finite element and the derivation of its stiffness matrix. The final part of the paper is devoted to giving a comparison of selected results that can be acquired either by layerwise finite element(Genson) or the other available theories in the literature.

Keywords: Laminated composite, finite element, zig-zag.

MSC number/numarası: 74S05.

**GELİŞTİRİLEN TABAKALI SONLU ELEMENLA KOMPOZİT PLAKLARIN LİNEER STATİK
ANALİZİ**

ÖZET

Bu makale tabakalı kompozit plakların lineer statik analizini gerçekleştirmek amacıyla geliştirilen tabakaduyarlı yeni bir sonlu eleman hakkında olup; birinci bölüm tabakalı kompozit plaklar üzerine literatürde mevcut teorilere ve bu teorilerin eksikliklerini gözden geçirmeye ayrılmıştır. İkinci bölüm; doğru gerilme ve şekildeğiştirme alanlarının elde edilmesi amacıyla dikkat edilmesi gereken bir anahtar nokta olan tabaka kalınlığı doğrultusunda deplasman alanlarının zig-zag biçimine sahip olma gerekliliğini açıklamaktadır. Üçüncü bölüm; geliştirilen sonlu elemanın açıklanmasına ve bu sonlu elemanın rijitlik matrisinin çıkarılışına ayrılmıştır. Makalenin son bölümünde; geliştirilen sonlu eleman (Genson) ile literatürde mevcut diğer teorilerin karşılaştırmalı sonuçlarına yer verilmiştir.

Anahtar Sözcükler: Tabakalı kompozit, sonlu eleman, zig-zag.

1. INTRODUCTION

Composite materials consist of two or more materials which together produce desirable properties such as stiffness, strength, corrosion resistance, thermal properties and fatigue life that cannot be achieved with any of the constituents alone. Fiber reinforced composite materials for structural applications are often made in the form of a thin layer, called lamina. Structural elements such as beams or plates are formed by stacking the layers to achieve desired strength and stiffness.

*Corresponding Author/Sorumlu Yazar: e-mail/e-ileti: hasim@itu.edu.tr, tel: (212) 559 64 63

In this section; the plate theories are explained from single layer structures through multilayered ones.

First studies in the plate and shell literature are grouped as Love First Approximation Theory (LFAT) by Kirchhoff (1850) and Love (1927) with an assumption that normal to the reference surface Ω remain normal in the deformed states and do not change in length. Likewise, Cauchy (1828) and Poisson (1829) have studied in thin shell assumptions which can be assigned to the first grouping. Reissner (1945) and Mindlin (1951) considered not only the work done by in-plane stresses but also the work done by transverse shear stresses in their studies and they are grouped as Love Second Approximation Theory (LSAT). Extensions of Kirchhoff-Love First Approximation Theory to layered structures are known as Classical Lamination Theory (Jones 1975). Applications of LSAT theories to multilayered structures are referred as the First Order Shear Deformation Theory (FSDT) by Whitney (1969). Thai and Choi (2013) proposed a simple FSDT for bending and free vibration analysis of laminates by making further simplifying assumptions to the existing FSDT, the number of unknowns and governing equations of the present FSDT are reduced by one. However, the drawback of FSDT comes from the representation of the constant transverse shear strains through laminate thickness and this discrepancy between the actual quadratic stress state and the constant stress state predicted by the first order theory is often corrected in computing transverse shear force resultants by multiplying the transverse stress integrals with a shear correction coefficient parameter.

Due to the need for shear correction coefficients used in the first order theory, higher order theories such as Reddy's theory (1997) are developed to have quadratic variation of the transverse shear strains and transverse shear stresses through each layer by expanding the displacement field in terms of the thickness coordinate up to any desired degree. However, its FEM implementation is somewhat hindered by the need to employ a C^1 continuous basis for the transverse displacement. Mendonça *et al.* (2013) have presented a method to model the bending problem of arbitrary anisotropic laminated composite plates, which allows an arbitrary C^k continuity under the kinematic hypothesis of the Third Order Plate Theory proposed by Reddy. Thai *et al.* (2012) have developed a finite element called NS-DSG3 based on a combination of node based smoothing discrete shear gap method with the Higher Order Shear Deformation Plate Theory (HSDT). Bhar *et al.* (2010) have brought out the significance of using the HSDT over the FSDT for analyzing laminated composite stiffened plates.

Following Reddy (1997), these types of theories such as CLT, FSDT or HSDT are grouped as Equivalent Single Layer Theories (ESLM) which have a number of unknown variables that are independent of the number of constitutive layers N_L . In addition to their inherent simplicity and low computational cost, the ESL models often provide sufficiently accurate description of global response for thin to moderately thick laminates, e.g., gross deflections, critical buckling loads. However, the ESL models are often incapable of accurately describing the state of stress and strain at the ply level near geometric and material discontinuities. In all equivalent single layer laminate theories based on assumed displacement fields and it is assumed that the displacements are continuous functions of the thickness coordinate. This in turn results in all stresses in ESL models are discontinuous at layer interfaces contrary to the actual transverse stress state.

2. MATERIAL PROPERTIES OF LAMINATED COMPOSITE PLATES

From Figure 1, it can be seen that a laminate is a collection of laminae which could have different material properties and fiber orientation to achieve the desired stiffness and thickness.

As a direct consequence of exhibition of different mechanical and physical properties in the thickness direction, layered composite plates show higher transverse shear and transverse normal stress deformability. ($G_{LT}/E_T \approx G_{TT}/E_T = 1/10 \sim 1/200$, where L denotes the fiber directions, while T is direction orthogonal to L) than single layer plates.

From Figure 2, it is noticed that laminated composites are made from two materials: a reinforcement material called fiber and a base material, called matrix material.

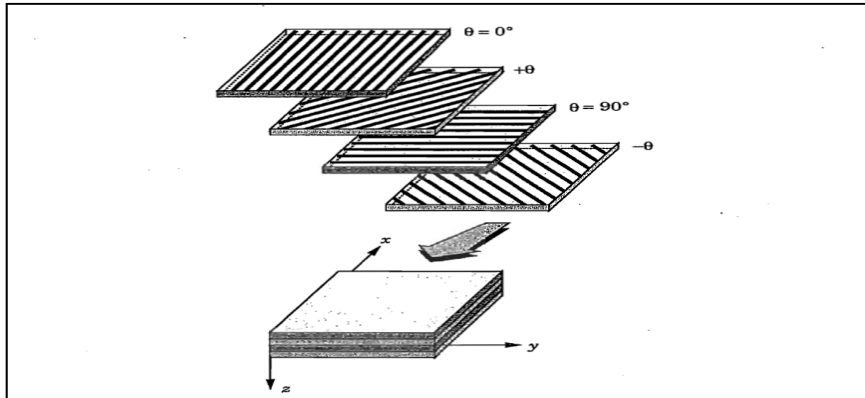


Figure 1. A laminate made up of plies with different fiber orientations

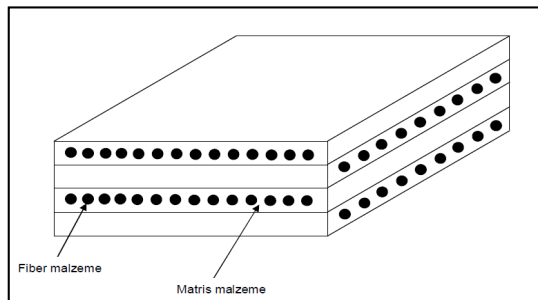


Figure 2. Fiber and matrix materials in laminated composite plates

The moduli and Poisson’s ratio of a laminated composite plate can be expressed in terms of the moduli, Poisson’s ratios and volume fractions of the matrix and fiber materials. Then it can be shown that the lamina engineering constants are given by

$$E_1 = E_f V_f + E_m V_m \quad \nu_{12} = V_f \nu_f + V_m \nu_m$$

$$E_2 = \frac{E_f E_m}{E_f V_m + E_m V_f} \quad G_{12} = \frac{G_f G_m}{G_f V_m + G_m V_f} \quad (1)$$

where E_1 is the longitudinal modulus, E_2 is transverse modulus, ν_{12} is the major Poisson’s ratio, G_{12} is the shear modulus, E_f is modulus of the fiber, E_m is modulus of the matrix, V_f is the fiber volume fraction, V_m is the matrix volume fraction, ν_f and ν_m are the Poisson’s ratios of the fiber and matrix respectively.

The stress and strain relationship of a typical orthotropic k th ($k = 1, \dots, n$) layer in the local co-ordinate system is

$$\begin{bmatrix} \sigma_{11} \\ \sigma_{22} \\ \sigma_{12} \end{bmatrix}^k = \begin{bmatrix} Q_{11} & Q_{12} & 0 \\ Q_{12} & Q_{22} & 0 \\ 0 & 0 & Q_{66} \end{bmatrix}^k \begin{bmatrix} \epsilon_{11} \\ \epsilon_{22} \\ \epsilon_{12} \end{bmatrix}^k ; \begin{bmatrix} \sigma_{23} \\ \sigma_{13} \end{bmatrix}^k = \begin{bmatrix} Q_{44} & 0 \\ 0 & Q_{55} \end{bmatrix}^k \begin{bmatrix} \epsilon_{23} \\ \epsilon_{13} \end{bmatrix}^k \quad (2)$$

in which

$$Q_{11}^k = \frac{E_1^k}{1-\theta_{12}^k\theta_{21}^k}, \quad Q_{12}^k = \frac{\theta_{12}^k E_2^k}{1-\theta_{12}^k\theta_{21}^k}, \quad Q_{22}^k = \frac{E_2^k}{1-\theta_{12}^k\theta_{21}^k}$$

$$Q_{66}^k = G_{12}^k, \quad Q_{44}^k = G_{23}^k, \quad Q_{55}^k = G_{13}^k \quad (3)$$

Von Karman (1910) linear strain displacement relation is in the following form.

$$\begin{bmatrix} \epsilon_x \\ \epsilon_y \\ \gamma_{xy} \end{bmatrix} = \begin{bmatrix} \frac{\partial u}{\partial x} \\ \frac{\partial v}{\partial y} \\ \frac{\partial u}{\partial y} + \frac{\partial v}{\partial x} \end{bmatrix} \quad \begin{bmatrix} \gamma_{yz} \\ \gamma_{xz} \end{bmatrix} = \begin{bmatrix} \frac{\partial v}{\partial z} + \frac{\partial w}{\partial y} \\ \frac{\partial u}{\partial z} + \frac{\partial w}{\partial x} \end{bmatrix} \quad (4)$$

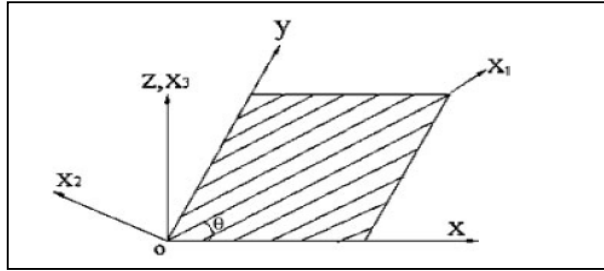


Figure 3. A lamina with global and material coordinate systems

From Figure 3, it can be seen that the laminate is made of several orthotropic layers, with their material axes oriented arbitrarily with respect to the laminate coordinates, the constitutive equations of each layer given in Eq. (2) must be transformed to the laminate coordinates (global-x,y,z).

For this aim, transformed stiffness matrix $[\bar{Q}]$ is formulated as

$$[\bar{Q}] = [T][Q][T]^T \quad (5)$$

where [T] is transformation matrix obtained by

$$[T] = \begin{bmatrix} \cos^2 \theta & \sin^2 \theta & -\sin 2\theta & 0 & 0 \\ \sin^2 \theta & \cos^2 \theta & \sin 2\theta & 0 & 0 \\ \sin \theta \cos \theta & -\sin \theta \cos \theta & \cos^2 \theta - \sin^2 \theta & 0 & 0 \\ 0 & 0 & 0 & \cos \theta & -\sin \theta \\ 0 & 0 & 0 & \sin \theta & \cos \theta \end{bmatrix} \quad (6)$$

By introducing Eq. (5) into Eq. (2), the stress-strain relationship becomes,

$$\begin{bmatrix} \sigma_x \\ \sigma_y \\ \tau_{xy} \end{bmatrix}_k = \begin{bmatrix} \bar{Q}_{11} & \bar{Q}_{12} & \bar{Q}_{16} \\ \bar{Q}_{12} & \bar{Q}_{22} & \bar{Q}_{26} \\ \bar{Q}_{16} & \bar{Q}_{26} & \bar{Q}_{66} \end{bmatrix} \begin{bmatrix} \epsilon_x \\ \epsilon_y \\ \gamma_{xy} \end{bmatrix}_k \quad \begin{bmatrix} \tau_{yz} \\ \tau_{xz} \end{bmatrix}_k = \begin{bmatrix} \bar{Q}_{44} & \bar{Q}_{45} \\ \bar{Q}_{54} & \bar{Q}_{55} \end{bmatrix} \begin{bmatrix} \gamma_{yz} \\ \gamma_{xz} \end{bmatrix}_k \quad (7)$$

2.1. Zigzag Effect

Transverse discontinuous mechanical properties cause displacement fields $\mathbf{u} = (u_1, u_2, u_3)$ in the thickness direction which can exhibit a rapid change of their slopes in correspondence to each layer interface. Figure 4 shows how the scenarios of displacement \mathbf{u} distributions in a laminated plate could appear in the exact solution or experiments. This displacement distribution is known as zigzag effect in the literature defined by Carrera (1997).

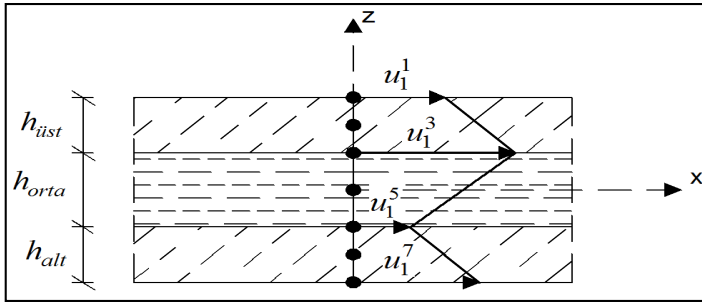


Figure 4. Zig-zag effect in the laminated composite plates

In all equivalent single layer laminate theories assume that the displacements are continuous functions of the thickness coordinate contrary to the actual zig-zag form of the laminated plates. Therefore; a possible, natural manner of including the zig-zag effect could be implemented by applying CLT, FSDT or TSDT at a layer level, that is, each layer is seen as an independent plate which is known as layerwise theory in the literature.

3. LAYERWISE FINITE ELEMENT FORMULATION

When the main emphasis of the analysis is to determine the overall global response of the laminated plates, for example, gross deflections, critical buckling loads, such global behavior can often be accurately determined using equivalent single layer laminate theories (ESL) especially for very thin laminates. As laminated composite materials undergo the transition from secondary structural components to primary critical structural components which are thicker, then the simple ESL theories are incapable of accurately determining the 3-D stress field at the ply level as a result of zig-zag effect explained in the previous section.

As can be seen in Fig. 5, a 3-D layerwise serendipity finite element which has four nodes (cubic) per side in plan and three nodes (quadratic) in the thickness direction is developed in this study.

The layerwise finite element has two in-plane degrees of freedom (u_{ij}, v_{ij}) ($I=1, \dots, 12$) ($j=u, o, a$) per plan and thickness nodes and a one (w) out of plane degrees of freedom which means $\epsilon_{zz} = 0$.

Figure 6 shows that a three layered layerwise finite element has a total of 180 nodal displacements per element.

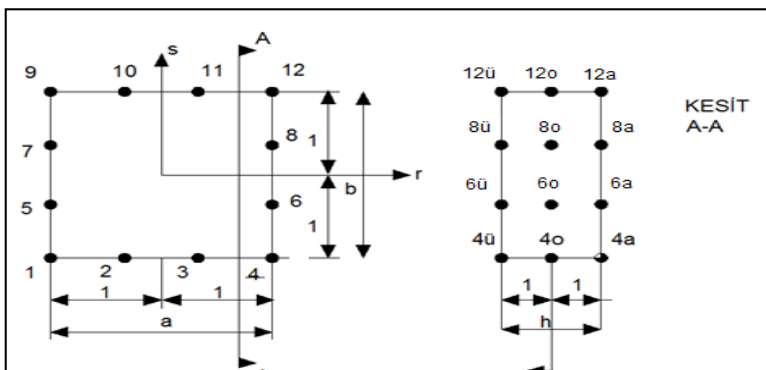


Figure 5. A 3-D layerwise finite element and node numbering

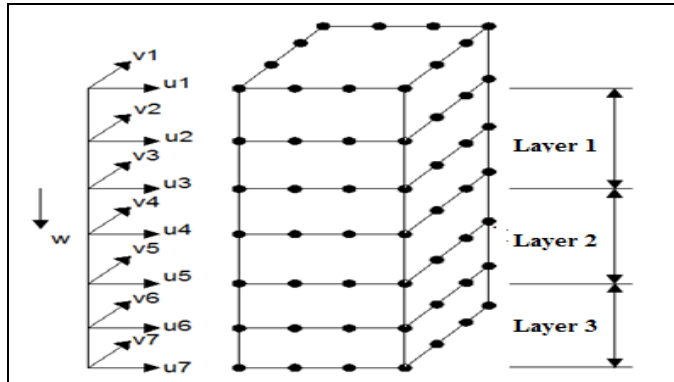


Figure 6. Nodal degrees of freedom in 3 layered layerwise finite element

Lagrange cubic interpolation functions which are given in Reddy (2005) are used in plan as follows:

$$\begin{aligned}
 N_a &= \frac{1}{32}(1+r_a r)(1+s_a s)[9(r^2+s^2)-10] ; (a=1,4,9,12) \\
 N_a &= \frac{9}{32}(1+9r_a r)(1+s_a s)(1-r^2) ; (a=2,3,10,11) \\
 N_a &= \frac{9}{32}(1+9s_a s)(1+r_a r)(1-s^2) ; (a=5,6,7,8)
 \end{aligned}
 \tag{8}$$

where r and s are local coordinates in plan. By separating r and s functions from each other, Eq. (8) becomes:

$$\begin{aligned}
 N_1(r, s) &= T_2(r)L_2(s) + L_2(r)T_2(s) - L_2(r)L_2(s) \\
 N_4(r, s) &= T_1(r)L_2(s) + L_1(r)T_2(s) - L_1(r)L_2(s) \\
 N_9(r, s) &= T_2(r)L_1(s) + L_2(r)T_1(s) - L_2(r)L_1(s) \\
 N_{12}(r, s) &= T_1(r)L_1(s) + L_1(r)T_1(s) - L_1(r)L_1(s) \\
 N_{11}(r, s) &= S_1(r)L_1(s) ; N_{10}(r, s) = S_2(r) L_1(s) \\
 N_3(r, s) &= S_1(r)L_2(s) ; N_2(r, s) = S_2(r)L_2(s) \\
 N_8(r, s) &= S_1(s)L_1(r) ; N_6(r, s) = S_2(s)L_1(r) \\
 N_7(r, s) &= S_1(s)L_2(r) ; N_5(r, s) = S_2(s)L_2(r)
 \end{aligned}
 \tag{9}$$

where $T_i, L_i, S_i (i=1,2)$ functions are defined as

$$\begin{aligned}
 T_1(r) &= \frac{-1}{16}(1-9r^2)(1+r) ; & T_2(r) &= \frac{-1}{16}(1-9r^2)(1-r) \\
 T_1(s) &= \frac{-1}{16}(1-9s^2)(1+s) ; & T_2(s) &= \frac{-1}{16}(1-9s^2)(1-s) \\
 S_1(r) &= \frac{9}{16}(1-r^2)(1+3r) ; & S_2(r) &= \frac{9}{16}(1-r^2)(1-3r) \\
 S_1(s) &= \frac{9}{16}(1-s^2)(1+3s) ; & S_2(s) &= \frac{9}{16}(1-s^2)(1-3s) \\
 L_1(r) &= \frac{1}{2}(1+r) ; & L_2(r) &= \frac{1}{2}(1-r)
 \end{aligned}
 \tag{10}$$

Quadratic interpolation functions in the thickness direction are obtained as follows:

$$\begin{aligned}
 \psi_{\bar{u}}(\zeta) &= \frac{1}{2} \zeta (1 + \zeta) \\
 \psi_a(\zeta) &= \frac{-1}{2} \zeta (1 - \zeta) \\
 \psi_o(\zeta) &= (1 - \zeta^2)
 \end{aligned}
 \tag{11}$$

where ζ is the local coordinate in the thickness direction. Displacement fields (u, v, w) could be obtained by using Eqs. (9-11). For a displacement state (i = 1, ... ,7) where only node 1 displacements exist in a one layered layerwise finite element, the displacement fields could be obtained by using interpolation functions as follows :

i=1 state	$u_{1\bar{u}} = 1$ state	$u = N_1(r, s)\psi_{\bar{u}}(\zeta)$	$v = 0$	$w = 0$
i=2 state	$v_{1\bar{u}} = 1$ state	$v = N_1(r, s)\psi_{\bar{u}}(\zeta)$	$u = 0$	$w = 0$
i=3 state	$u_{1a} = 1$ state	$u = N_1(r, s)\psi_a(\zeta)$	$v = 0$	$w = 0$
i=4 state	$v_{1a} = 1$ state	$v = N_1(r, s)\psi_a(\zeta)$	$u = 0$	$w = 0$
i=5 state	$u_{1o} = 1$ state	$u = N_1(r, s)\psi_o(\zeta)$	$v = 0$	$w = 0$
i=6 state	$v_{1o} = 1$ state	$v = N_1(r, s)\psi_o(\zeta)$	$u = 0$	$w = 0$
i=7 state	$w_1 = 1$ state	$w = N_1(r, s)$	$u = 0$	$v = 0$

3.1. First Order Stiffness Matrix of the Layerwise Element

According to the principle of virtual displacement (PVD), stiffness matrix terms (k_{ij}) could be obtained by the work done by the stresses of the ith displacement state with the strains of the jth state such as:

$$k_{ij} = \int_{-h/2}^{h/2} \int_{-b/2}^{b/2} \int_{-a/2}^{a/2} (\sigma_{xi} \epsilon_{xj} + \sigma_{yi} \epsilon_{yj} + \tau_{xyi} \gamma_{xyj} + \tau_{xzi} \gamma_{xzj} + \tau_{yzi} \gamma_{yzj}) dx dy dz \tag{12}$$

By substituting Eqs. (4 – 7) in Eq. (12) and for i = j = 1 state, Eq. (12) yields,

$$\begin{aligned}
 k_{11} &= \int_{-h/2}^{h/2} \int_{-b/2}^{b/2} \int_{-a/2}^{a/2} \left(Q_{11} \frac{\partial u_1(r, s)}{\partial x} \frac{\partial u_1(r, s)}{\partial x} + Q_{16} \frac{\partial u_1(r, s)}{\partial y} \frac{\partial u_1(r, s)}{\partial x} \right. \\
 &+ \left. Q_{16} \frac{\partial u_1(r, s)}{\partial x} \frac{\partial u_1(r, s)}{\partial y} + Q_{66} \frac{\partial u_1(r, s)}{\partial y} \frac{\partial u_1(r, s)}{\partial y} + Q_{55} \frac{\partial u_1(r, s)}{\partial z} \frac{\partial u_1(r, s)}{\partial z} \right) dx dy dz
 \end{aligned}
 \tag{13}$$

Displacement fields in Eq. (13) could be rearranged in form of interpolation functions by considering Eq. (11) for i = 1 state yields,

$$\begin{aligned}
 k_{11} &= \int_{-h/2}^{h/2} \int_{-b/2}^{b/2} \int_{-a/2}^{a/2} \left[Q_{11} \frac{\partial N_1(r, s)}{\partial x} \psi_{\bar{u}}(\zeta) \frac{\partial N_1(r, s)}{\partial x} \psi_{\bar{u}}(\zeta) + Q_{16} \frac{\partial N_1(r, s)}{\partial y} \psi_{\bar{u}}(\zeta) \frac{\partial N_1(r, s)}{\partial x} \psi_{\bar{u}}(\zeta) \right. \\
 &+ \left. Q_{16} \frac{\partial N_1(r, s)}{\partial x} \psi_{\bar{u}}(\zeta) \frac{\partial N_1(r, s)}{\partial y} \psi_{\bar{u}}(\zeta) + Q_{66} \frac{\partial N_1(r, s)}{\partial y} \psi_{\bar{u}}(\zeta) \frac{\partial N_1(r, s)}{\partial y} \psi_{\bar{u}}(\zeta) \right. \\
 &+ \left. Q_{55} N_1(r, s) \frac{d\psi_{\bar{u}}(\zeta)}{dz} N_1(r, s) \frac{d\psi_{\bar{u}}(\zeta)}{dz} \right] dx dy dz
 \end{aligned}
 \tag{14}$$

As can be seen from Eq. (14), integrand contains derivatives with respect to the global coordinates (x, y, z) however; interpolation (shape) functions are written in local coordinate system (r, s, ζ). The relation $\frac{\partial N_1(r, s)}{\partial x}$ and $\frac{\partial N_1(r, s)}{\partial y}$ to $\frac{\partial N_1}{\partial r}$ and $\frac{\partial N_1}{\partial s}$ is obtained by :

$$\begin{bmatrix} \frac{\partial N_1(r, s)}{\partial x} \\ \frac{\partial N_1(r, s)}{\partial y} \end{bmatrix} = [J]_{xy}^{-1} \begin{bmatrix} \frac{\partial N_1(r, s)}{\partial r} \\ \frac{\partial N_1(r, s)}{\partial s} \end{bmatrix} = \begin{bmatrix} J_{11}^* & J_{12}^* \\ J_{21}^* & J_{22}^* \end{bmatrix} \begin{bmatrix} \frac{\partial N_1(r, s)}{\partial r} \\ \frac{\partial N_1(r, s)}{\partial s} \end{bmatrix}
 \tag{15}$$

where [J] is called the Jacobian matrix of the transformation :

$$[J]_{xy} = \begin{bmatrix} \frac{\partial N_1}{\partial r} & \frac{\partial N_2}{\partial r} & \dots & \frac{\partial N_{m=12}}{\partial r} \\ \frac{\partial N_1}{\partial s} & \frac{\partial N_2}{\partial s} & \dots & \frac{\partial N_{m=12}}{\partial s} \end{bmatrix} \begin{bmatrix} x_1 & y_1 \\ x_2 & y_2 \\ \vdots & \vdots \\ x_{m=12} & y_{m=12} \end{bmatrix} \tag{16}$$

The element area $dA = dx dy$ in Eq. (14) is also transformed to

$$dx dy = \det(J_{xy}) dr ds \tag{17}$$

By considering Eqs. (15 - 17) in Eq. (14) yields,

$$k_{11} = \int_{-h/2}^{h/2} \int_{-1}^1 \int_{-1}^1 \left[\overline{Q}_{11} \left(J_{11}^* \frac{\partial N_1(r,s)}{\partial r} + J_{12}^* \frac{\partial N_1(r,s)}{\partial s} \right) \left(J_{11}^* \frac{\partial N_1(r,s)}{\partial r} + J_{12}^* \frac{\partial N_1(r,s)}{\partial s} \right) \psi_{\bar{u}}(\zeta) \psi_{\bar{u}}(\zeta) \right. \\ + \overline{Q}_{16} \left(J_{21}^* \frac{\partial N_1(r,s)}{\partial r} + J_{22}^* \frac{\partial N_1(r,s)}{\partial s} \right) \psi_{\bar{u}}(\zeta) \left(J_{11}^* \frac{\partial N_1(r,s)}{\partial r} + J_{12}^* \frac{\partial N_1(r,s)}{\partial s} \right) \psi_{\bar{u}}(\zeta) \\ + \overline{Q}_{16} \left(J_{11}^* \frac{\partial N_1(r,s)}{\partial r} + J_{12}^* \frac{\partial N_1(r,s)}{\partial s} \right) \psi_{\bar{u}}(\zeta) \left(J_{21}^* \frac{\partial N_1(r,s)}{\partial r} + J_{22}^* \frac{\partial N_1(r,s)}{\partial s} \right) \psi_{\bar{u}}(\zeta) \\ + \overline{Q}_{66} \left(J_{21}^* \frac{\partial N_1(r,s)}{\partial r} + J_{22}^* \frac{\partial N_1(r,s)}{\partial s} \right) \psi_{\bar{u}}(\zeta) \left(J_{21}^* \frac{\partial N_1(r,s)}{\partial r} + J_{22}^* \frac{\partial N_1(r,s)}{\partial s} \right) \psi_{\bar{u}}(\zeta) \\ \left. + \overline{Q}_{55} N_1(r,s) J_z^{-1} \frac{d\psi_{\bar{u}}(\zeta)}{d\zeta} N_1(r,s) J_z^{-1} \frac{d\psi_{\bar{u}}(\zeta)}{d\zeta} \right] \det(J_{xy}) dr ds dz \tag{18}$$

Integration through thickness (z) direction is calculated using Table 1.

Table 1. $\int_{-h/2}^{h/2} X Y dz$

X-Y	$\psi_{\bar{u}}$	ψ_a	ψ_o	$\psi'_{\bar{u}}$	ψ'_a	ψ'_o
$\psi_{\bar{u}}$	$\frac{2h}{15}$	$\frac{-h}{30}$	$\frac{h}{15}$	$\frac{1}{2}$	$\frac{1}{6}$	$\frac{-2}{3}$
ψ_a		$\frac{2h}{15}$	$\frac{h}{15}$	$\frac{-1}{6}$	$\frac{-1}{2}$	$\frac{2}{3}$
ψ_o			$\frac{8h}{15}$	$\frac{2}{3}$	$\frac{-2}{3}$	0
$\psi'_{\bar{u}}$				$\frac{7}{3h}$	$\frac{1}{3h}$	$\frac{-8}{3h}$

The area integration of the stiffness matrix in Eq. (18) is evaluated by numerical integration using the Gauss quadrature formula with 4x4 sampling points.

4. NUMERICAL RESULTS

4.1. Square Plates

As can be seen in Fig. 7, simply supported [0/90/0] and [0/90/90/0] layered cross ply square plates with length L and thickness h subjected to doubly sinusoidal loading $q = q_0 \sin(\frac{\pi x}{L}) \sin(\frac{\pi y}{L})$ are studied. The material properties are: $E_1/E_2 = 25.0$, $G_{12} = G_{13} = 0.5E_2$, $G_{23} = 0.2E_2$, $\nu_{12} = \nu_{13} = 0.25$. The whole plate is modeled with 6 x 6 meshes.

Calculations are performed for the normalized central deflection $\bar{w} = w_0 \left(\frac{L}{2}, \frac{L}{2} \right) \left(\frac{E_2 h^3}{L^4 q_0} \right)$, normalized in plane stresses $\bar{\sigma}_{xx} = \sigma_{xx} \left(\frac{h^2}{L^2 q_0} \right)$ at point $(L/2, L/2, h/2)$, $\bar{\sigma}_{yy} = \sigma_{yy} \left(\frac{h^2}{L^2 q_0} \right)$ at point $(L/2, L/2, h/4)$, normalized shear stresses $\bar{\sigma}_{yz} = \sigma_{yz} \left(\frac{h}{L q_0} \right)$ at point $(L/2, 0, 0)$, $\bar{\sigma}_{xz} = \sigma_{xz} \left(\frac{h}{L q_0} \right)$ at point $(0, L/2, 0)$ for the 3-layer plate and the 4-layer plate.

The results are compared with the exact solutions from Pagano and Hatfield (1972) and Pagano (1969) and those obtained from layerwise finite element (Genson) with 6x6 mesh in Table 2 for the 3 layered square plate and in Table 3 for the 4 layered square plate.

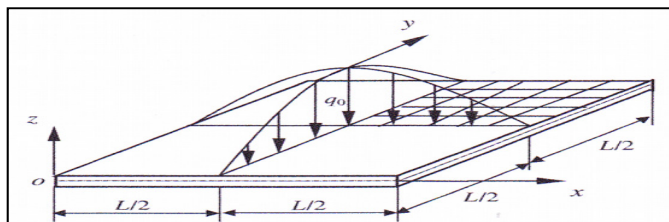


Figure 7. Simply supported cross ply 3 and 4-layer square plates subjected to doubly sinusoidal loading

Table 2. Normalized central deflection and stresses of a simply supported 3-layer square plate under doubly sinusoidal loading

L/h	Variable	Genson Layerwise	ELS [†]	TSDT	FSDT				CLPT
					K = 1	K = 5/6	K = 3/4	K = 1/2	
4	$\bar{w} \times 10^2$	2.065	-----	1.9218	1.5681	1.7758	1.9122	2.5770	0.4313
	$\bar{\sigma}_{xx}$	0.789	0.755	0.7345	0.4475	0.4370	0.4308	0.4065	0.5387
	$(\bar{\sigma}_{yz})$	0.180	0.217	0.1832	0.1227	0.1561	0.1793	0.3030	-----
	*	-----	-----	0.2086	0.1850	0.1968	0.2038	0.2311	0.0823
10	$\bar{w} \times 10^2$	0.765	-----	0.7125	0.6306	0.6693	0.6949	0.8210	0.4313
	$\bar{\sigma}_{xx}$	0.599	0.590	0.5684	0.5172	0.5134	0.5109	0.4993	0.5387
	$(\bar{\sigma}_{yz})$	0.108	0.123	0.1033	0.0735	0.0915	0.1039	0.1723	-----
		-----	-----	0.1167	0.1065	0.1108	0.1136	0.1267	0.0823
100	$\bar{w} \times 10^2$	0.434	-----	0.4342	0.4333	0.4337	0.4340	0.4353	0.4313
	$\bar{\sigma}_{xx}$	0.542	0.552	0.5390	0.5385	0.5384	0.5384	0.5382	0.5387
	$(\bar{\sigma}_{yz})$	0.147	0.094	0.0750	0.0586	0.0703	0.0782	0.1174	-----

[†] 3-D elasticity solution of Pagano (1969).

* The second line corresponds to stresses computed from 3-D elasticity equilibrium equations.

Table 3. Normalized central deflection and stresses of a simply supported 4 layer square plate under sinusoidal loading

L/h	Source	$\bar{w} \times 10^2$	$\bar{\sigma}_{xx}$	$\bar{\sigma}_{yy}$	$\bar{\sigma}_{yz}$	$\bar{\sigma}_{xz}$
4	Genson	1.992	0.715	0.686	0.340	0.228
	ELS [§]	1.954	0.720	0.663	0.292	0.219
	TSDT	1.894	0.665	0.632	0.239	0.206
					0.298	0.231**
FSDT	1.710	0.406	0.576	0.196	0.140	
				0.280	0.269	
10	Genson	0.747	0.568	0.406	0.235	0.312
	ELS	0.743	0.559	0.401	0.196	0.301
	TSDT	0.715	0.546	0.389	0.153	0.264
					0.192	0.307
FSDT	0.663	0.4989	0.361	0.130	0.167	
				0.181	0.318	
20	Genson	0.517	0.548	0.310	0.197	0.338
	ELS	0.517	0.543	0.308	0.156	0.328
	TSDT	0.506	0.539	0.304	0.123	0.282
					0.154	0.330
FSDT	0.491	0.527	0.296	0.109	0.175	
				0.150	0.333	
100	Genson	0.434	0.542	0.274	0.242	0.375
	ELS	0.438	0.539	0.276	0.141	0.337
	TSDT	0.434	0.539	0.271	0.112	0.290
					0.139	0.339
FSDT	0.434	0.538	0.270	0.101	0.178	

4.2. Circular Plates

As can be seen in Figure 8, isotropic and orthotropic single layer circular plates with radius $r = 6$ [m] subjected to uniform pressure are studied. Plates are analyzed using both simply supported and clamped boundary conditions. Isotropic material properties: $E_1 = E_2 = 30 \times 10^6$ (psi), $\nu = 0.25$, $G_{xy} = G_{xz} = G_{yz} = \frac{E}{2(1+\nu)} = 12 \times 10^6$ (psi) Orthotropic material properties: $E_1 = 30 \times 10^6$ (psi), $E_2 = 0.75 \times 10^6$ (psi), $\nu_{12} = 0.25$, $\nu_{21} = 6.25 \times 10^{-3}$, $G_{xy} = G_{xz} = 0.45 \times 10^6$ (psi), $G_{yz} = 0.375 \times 10^6$ (psi). The whole plate is modeled with 20 elements. The material fibers angle $\theta = 0$ with respect to the global x axis is assumed.

The results of isotrop one layered circular plates for clamped and simply supported boundary conditions under uniform pressure are compared with the exact solutions from Ugural(1981) and those obtained from layerwise finite element (Genson) in Figs. 9-10.

[§] 3-D elasticity solution of Pagano and Hatfield (1972).

** Equilibrium -derived stresses.

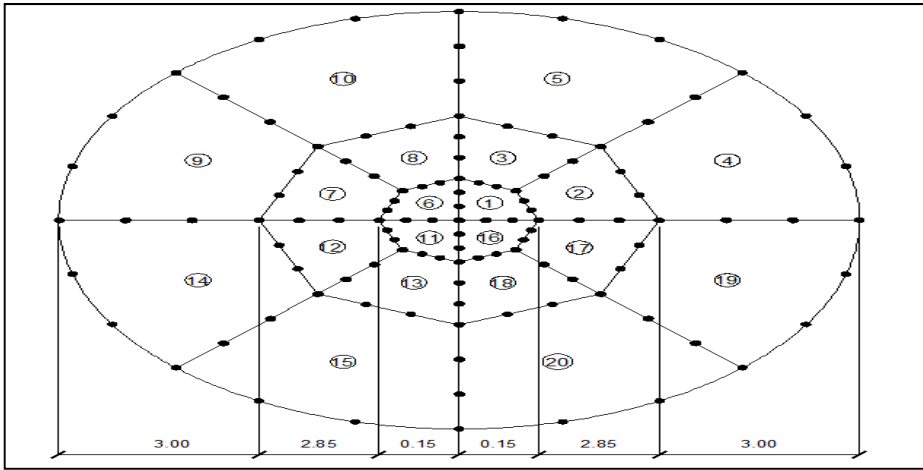


Figure 8. Axisymmetric single layer circular plate

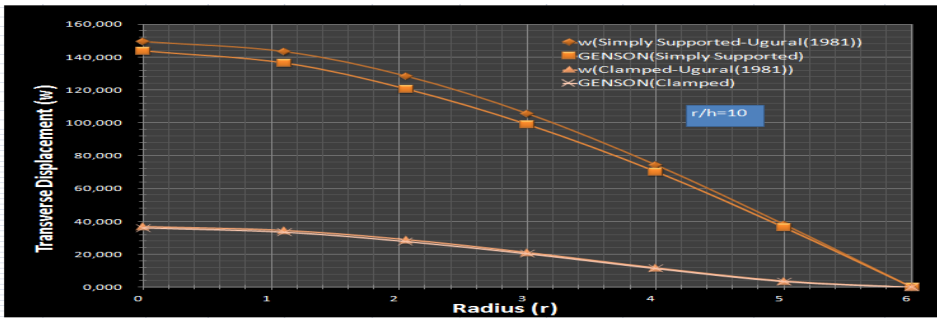


Figure 9. Transverse displacements of single layer isotropic circular plate under uniform pressure ($r/h = 10$)

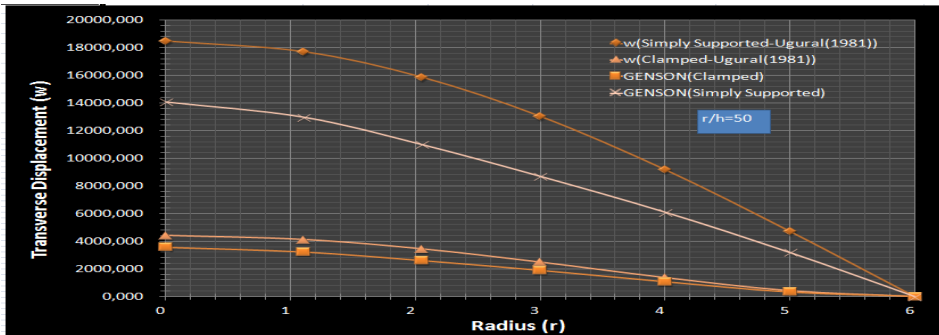


Figure 10. Transverse displacements of single layer isotropic circular plate under uniform pressure ($r/h = 50$)

Table 4. Normalized central deflection of one layered clamped circular plates

Normalized center deflection, w^*		
Number of elements		
a/h	12	20(GENSON)
100	0.1159	0.1160
50	0.1242	0.1280
25	0.1373	0.1409

The results of orthotropic single layer clamped circular plates under uniform pressure q_0 for various plate aspect ratios (r/h) are compared with the finite element solutions from Wilt *et al.* (1990) in Table 4. Note that the quantities in the following tables are normalized center deflections, w^* , i.e. $w^* = wD/q_0a^4$ where $D=3(D_{11} + D_{22}) + 2(D_{12} + 2D_{66})$ and D_{11} , D_{22} , D_{12} and D_{66} are bending stiffnesses.

The results of orthotropic single layer clamped circular plates for various plate aspect ratios (r/h) under uniform pressure are also compared with closed form solution by Leiknitski (1968) and Murthy and Lakshminarayana (1984) in Figs. 11-12.

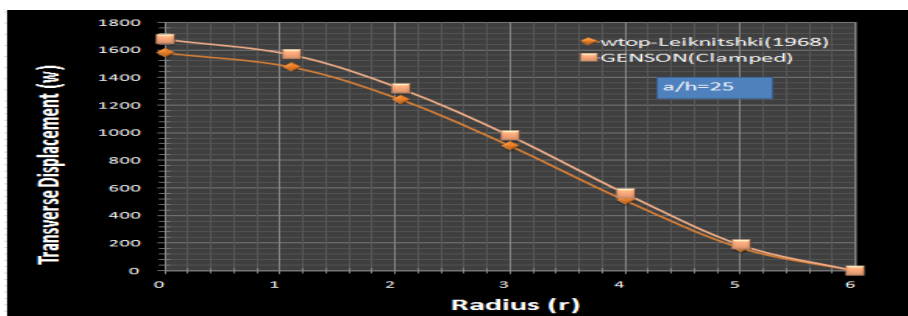


Figure 11. Transverse displacements of single layer orthotropic circular plate under uniform pressure ($r/h = 25$)

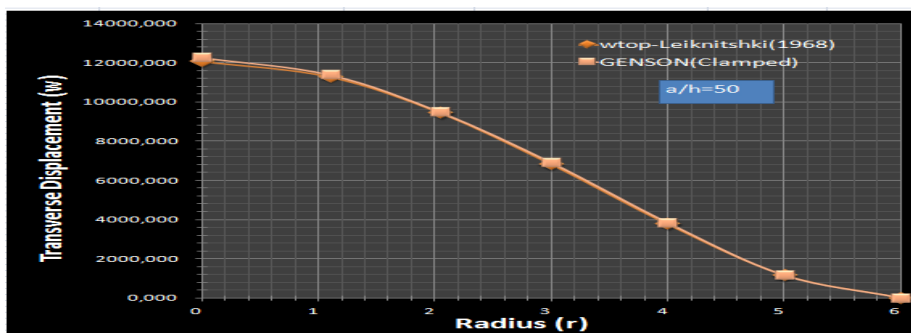


Figure 12. Transverse displacements of single layer orthotropic circular plate under uniform pressure ($r/h = 50$)

5. CONCLUSIONS

A 3-D layerwise serendipity finite element which has four nodes (cubic) per side in plan and three nodes (quadratic) in the thickness direction is developed in this study to analyze the linear static response of the laminated plates. The elements are simple, shear locking free and fast convergent. Numerical results show that the present elements are accurate and efficient compared

with the elasticity solutions in the literature for isotropic or orthotropic square and circular laminated plates.

REFERENCES / KAYNAKLAR

- [1] Kirchhoff G., "Über das Gleichgewicht und die Bewegung einer elastischen Scheibe", *J. Angew Math.*, 40, 51-88, 1850.
- [2] Bhar, A., Phoenix, S.S. and Satsangi, S.K. (2010), "Finite element analysis of laminated composite stiffened plates using FSDT and HSDT: A comparative perspective", *Composite Structures.*, 92, 312-321.
- [3] Love, A.E.H. (1927), *The Mathematical Theory of Elasticity*, (4th Edition), Cambridge Univ Press, Cambridge.
- [4] Cauchy, A.L. (1828), "Sur l'équilibre et le mouvement d'une plaque solide", *Exercices de Mathématique.*, 3, 328-355.
- [5] Thai, C.H., Tran L.C., Tran D.T., Nguyen-Thoi, T. and Nguyen-Xuan, H. (2012), "Analysis of laminated composite plates using higher order shear deformation plate theory and node based smoothed discrete shear gap method", *Applied Mathematical Modelling.*, 36, 5657-5677.
- [6] Poisson, S.D. (1829), "Memoire sur l'équilibre et le mouvement des corps élastique", *Mem. Acad. Sci.*, 8, 357.
- [7] Reissner, E. (1945), "The effect of transverse shear deformation on the bending of elastic plates", *ASME J. Appl. Mech.*, 12, 69-76.
- [8] Mindlin, R.D. (1951), "Influence of rotary inertia and shear in flexural motions of isotropic elastic plates", *ASME J. Appl. Mech.*, 18, 1031-1036.
- [9] Mendonça, P.T.R., Barcellos, C.S. and Torres, D.A.F. (2013), "Robust C^k/C^0 generalized FEM approximations for higher-order conformity requirements: Application to Reddy's HSDT model for anisotropic laminated plates", *Composite Structures.*, 96, 332-345.
- [10] Jones, R.M. (1975), *Mechanics of Composite Materials*, Mc Graw Hill, New York.
- [11] Whitney, J. (1969), "The effects of transverse shear deformation on the bending of laminated plates", *J. Compos. Mater.*, 3, 534-547.
- [12] Reddy, J.N. (1997), *Mechanics of Laminated Composite Plates. Theory and Analysis*, CRC Press, Boca Raton FL.
- [13] Von Karman, T. (1910), "Festigkeitsprobleme in Maschinenbau", *Encyklopadie der Mathematischen Wissenschaften*, 4, 311-385.
- [14] Pagano, N.J. and Hatfield, S.J. (1972), "Elastic Behavior of Multilayered Bidirectional Composites", *AIAA Journal*, 10, 931-933.
- [15] Pagano, N.J. (1969), "Exact Solutions for Composite Laminates in Cylindrical Bending", *Journal of Composite Materials*, 3, 398-411.
- [16] Carrera, E. and Kröplin, B. (1997), "Zig-zag and interlaminar equilibria effects in large deflection and postbuckling analysis of multilayered plates", *Mechanics of Composite Materials and Structures*, 4, 69-94.
- [17] Reddy, J.N. (2005), *An Introduction to the Finite Element Method*, Mc Graw Hill, NY.
- [18] Ugural, A.C. (1981), *Stresses in Plates and Shells*, Mc Graw Hill, New York.
- [19] Wilt, T.E., Saleeb, A.F. and Chang, T.Y. (1990), "A mixed element for laminated plates and shells", *Computers and Structures.*, 37, 597-611.
- [20] Leiknitschki, S. (1968), *Anisotropic Plates*.
- [21] Huu-Tai, T. and Dong-Ho, C. (2013), "A simple first order shear deformation theory for laminated composite plates", *Composite Structures*, 106, 754-763
- [22] Murthy, S.S. and Lakshminarayana, H.V. (1984), "A shear flexible triangular finite element model for laminated composite plates", *Journal for Numerical Methods in Engineering*, 20, 591-623.